Journal
of Achievements in Materials
and Manufacturing Engineering

VOLUME 44
ISSUE 2
February
2011

Hydrogen storage alloys prepared by high-energy milling

M. Staszewski [a,*], A. Sierczyńska [b], M. Kamińska [a], M. Osadnik [a], M. Czepelak [a], P. Swoboda [b]

[a] Institute of Non-Ferrous Metals, ul. Sowińskiego 5, 44-100 Gliwice, Poland
[b] Institute of Non-Ferrous Metals Division in Poznan, Central Laboratory of Batteries and Cells, ul. Forteczna 12, 61-362 Poznań, Poland
* Corresponding author: E-mail address: mariusz.staszewski@imn.gliwice.pl

Received 03.12.2010; published in revised form 01.02.2011

Materials

ABSTRACT

Purpose: The aim of this work was to investigate an efficiency of high-energy milling, as a method to obtain hydrogen storage alloys with good properties.

Design/methodology/approach: Two classes of the alloys were studied: AB_2 type with atomic composition of $(Ti_{0.5}Zr_{0.5})(V_{0.68}Mn_{0.68}Cr_{0.34}Ni_{0.7})$ and AB_5 type with atomic composition of $(Ce_{0.63}La_{0.37})(Ni_{3.55}Al_{0.3}Mn_{0.4}Co_{0.75})$.The materials were prepared by arc melting and initially pulverized and afterwards subjected to wet milling process in a planetary mill.

Findings: Both initially obtained alloys had proper, single phase structure of hexagonal symmetry. However their elemental composition was greatly inhomogeneous. High-energy milling causes both homogenization of the composition and severe fragmentation of the powder particles, which after milling have mean diameter of about 3 µm (AB_2 alloy) and below 2 µm (AB_5 alloy). The morphology of obtained powders reveals that they tend to form agglomerates consisting of large number of crystallites. Mean crystallite sizes after milling are of about 4.5 nm and of 20 nm, respectively. The specific surface of the powders, measured using BET method, equals 8.74 m^2/g and 2.70 m^2/g, respectively.

Research limitations/implications: The results provide the information on the possibility of obtaining hydrogen storage alloys by high-energy milling and on the transformations taking place as a result of this process.

Practical implications: The obtained powders can be used to produce the elements of hydrogen-nickel batteries and fuel cells, providing improved properties; especially extreme rise of the specific surface of the hydrogen storage material, in compare to the standard methods.

Originality/value: New method for preparation of hydrogen storage alloys by means of high-energy milling technique has been successfully tested.

Keywords: Metallic alloys; Hydrogen storage materials; High-energy milling; X-ray Phase Analysis; Microanalysis; Physical properties

Reference to this paper should be given in the following way:

M. Staszewski, A. Sierczyńska, M. Kamińska, M. Osadnik, M. Czepelak, P. Swoboda, Hydrogen storage alloys prepared by high-energy milling, Journal of Achievements in Materials and Manufacturing Engineering 44/2 (2011) 154-160.

1. Introduction

Hydrogen storage alloys are used as a working material of the negative electrode in nickel-metal hydride batteries. They can also be used as a component of fuel cells or other “clean” energy sources. Hydrogen as a fuel, despite it numerous advantages, is hard to store or transport [1-4]. Its usage, in a pressurized gaseous form, has many limitations and is mostly unprofitable. Therefore, there is still a need to design and create new materials, in which the dissolve and release of the hydrogen is easy and cheap to achieve [3-9]. Those materials are sometimes based on carbon structures like nanotubes or fullerenes [3] or more often, on metal alloys with crystalline structure that enables the hydrogen atoms penetrate the alloy [2-15].

Good abilities are show by the generation of one-phase hydrogen storage alloys. Those alloys appear usually in two main types. The AB_2 type intermetallic Laves phase, for example Mg_2Ni compound [6] or multicomponent alloys such as $(Zr,Ti)(Cr,Mn,V,Ni)_2$ [7], or the AB_5 type Haucke phase, mostly different modifications of $LaNi_5$ compound. Those modifications are mostly done by substituting the La atoms with different lanthanides, magnesium or titanium, and the Ni atom with cobalt, iron, chromium, manganese or aluminum [8,10-16].

Hydrogen storage alloys are tested and used in commercial production for many years [2]. However the methods of acquiring those alloys are still being improved and developed. New possibilities are created by using, for the milling process, new generation of high-energy planetary mills. Those mills can achieve rotation rate of 1100 rpm [16]. To compare - in conventional mill of this type, the usual rate of milling was about 90 to 360 rpm [17]. Because of those bigger rpm rates, the kinetic energy of milling is also very high. This should lead to extremely strong, and not acquired before, size reduction of the grinded material. This reduction manifest in small crystallite size and big surface development of the treated material.

The size of few nanometers for the crystalline structure, allow the milled material to show prosperities not acquirable for coarse-grained materials [18,19]. Also the size of the surface area of material is important. Due to the fact that the time of absorption and desorption of hydrogen is limited by the distance from the surface to the core of the material - the grade of the surface development is the next most important thing for the performance of those materials. Therefore there is still a need for examine the properties of the nanocrystalline hydrogen storage alloys [20-24], acquired by still developed methods of manufacturing: rapid solidification, mechanical alloying, reactive milling or by high-energy milling [17,25-27].

2. Experiments

2.1. Characteristic of tested alloys

The high-energy milling method was conducted on the two different hydrogen storage alloy types, marked SX 1 and SX 3.

The SX 1 alloy was an AB_2 (Laves phase) type. In this structure, the A atoms were Ti and Zr in equal amount, and the B atoms were: Cr, Mn, Ni and V. This alloy was a intermetallic compound with approximate chemical composition of $(Ti_{0,5}Zr_{0,5})(V_{0,68}Mn_{0,68}Cr_{0,34}Ni_{0,70})$. The expected crystalline structure is hexagonal type P63/mmc with approximate lattice parameters of **a** = 0.499 nm and **c** = 0.816 nm.

The SX 3 alloy was an AB_5 (Haucke phase) type. The A atoms were lanthanides, mostly Ce and La in proportion of 63:37, and the B atoms were Ni, Al, Mn and Co. The approximate chemical composition of this intermetallic compound is $Mm(Ni_{3,55}Al_{0,3}Mn_{0,4}Co_{0,75})$ and it was also an expected hexagonal crystalline structure of a P6/mmm type. The lattice parameters of the base compound $LaNi_5$ are: **a** = 0.5017 nm, **c** = 0.3987 nm (PDF#1-72-9767 [28]). The Mm symbol denotes misch metal as one alloy component without any separation to elements which it was composed of.

2.2. Arc-melting conditions

The alloys were prepared by an arc melting method carried out in an Bühler arc furnace, in argon atmosphere using a water-cooled copper crucible. The alloys were prepared using the mixture of pure metals (with minimal purity of 99.8% in mass). The mixture of metal components was prepared in an inert atmosphere. Before the melting procedure, the sample was additionally degassed three times by achieving vacuum in the arc furnace chamber, after that the chamber was filled with argon. The smelting process was also carried out in multistage way. The metal components mixture was melted in 6-stage way, in every stage the current was changed from 30 to 100 A. After each melt stage, the sample was cooled in argon atmosphere, and recast to achieve the best homogenization of the metals in the sample. Material acquired this way was then mechanically crumbled on a hydraulic press. The composition of obtained alloys, corresponding to the mass proportion of pure materials used to prepare the mixture, is shown in the Table 1.

Table 1.
Chemical compositions of investigated alloys (mass %)

Element	Zr	Ti	Mn	V	Cr	Ni	Mm	Al	Co
SX 1	22.8	12.0	18.6	17.3	8.8	20.5	-	-	-
SX 3	-	-	7.7	-	-	44.2	32.9	1.3	13.9

2.3. High-energy milling conditions

The previously crumbled material was milled in planetary ball mill Fritsch Pulverisette 7 Premium Line, in tungsten carbide vessel with tungsten carbide milling balls. According to the producer information, the energy of milling for this type of mill, is approximately one and a half higher than the energy of conventional planetary mills. The milling process was carried out in ethanol, for 1 hour with following parameters of the mill: rotation speed of 800 rpm, ball-to-powder mass ratio of 6:1 and diameter of the balls equal to 5 mm.

Due to overheating the mill, during working, especially when milling the SX 1 alloy, the milling was conducted in a multistage way. Each stage lasted from few to several minutes. Each time when the mill temperature exceeded the value of 70°C the milling process was stopped, and restarted after cooling down the mill surface to the ambient temperature. The cell was filled and emptied in argon atmosphere in the glove box. Also the samples were stored under argon.

2.4. The methods of analysis

X-ray diffraction of the alloy structure was made by Seifert-FPM XRD 7 diffractometer with the CoK_{α} specific radiation. The measurement was done by step scan, were the length of the step was 0.04^{O} 2Θ, and the time of scan step was 2s. The identification of phase composition was made based on Seifert software and the PDF-2 (2007) catalog data, from the International Centre for Diffraction Data (ICDD) [28]. The crystallite size was defined by Scherrer method, based on diffraction line broadening. The results of the X-ray diffraction are shown on the Figs 1 and 2.

To examine the morphology of the obtained powders, the secondary electron imaging (SEI) and COMPO imaging techniques were used to observe the microstructure. To examine the homogenization process the analysis, both quantitative and qualitative, of elements in microareas was done with the WDS method. The JEOL JXA 8230 X-ray microanalyzer was used for this analysis. The Figs 3 and 4 show the microstructure of the source material, and the morphology of the obtained powders. The local analysis results are shown in the Tables 2-5. The determined amounts of elements are the mean value acquired from 5 to 10 measurement points.

The densities were measured on the Micromeritics Accupyc 1330 system. The specific surface area was defined by the gas absorption (BET) technique on the Micromeritics Gemini 2360 apparatus. The grain size was measured by laser diffraction on the Fritsch Analysette 22 Nanotec analyzer. The results of those tests are shown in the Table 6.

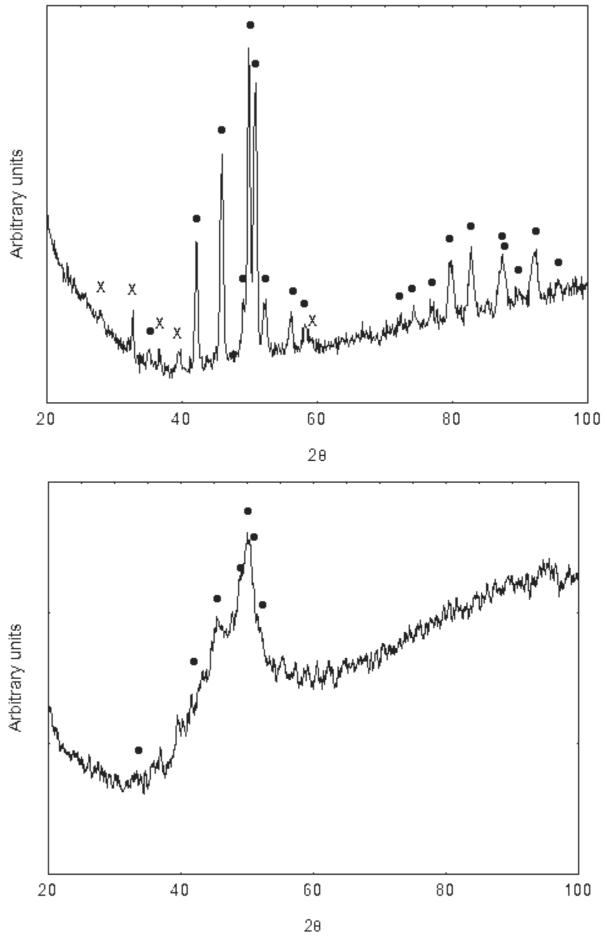

Fig. 1. X-ray diffraction patterns of SX 1 alloy: in basic state (higher) and after milling (lower). Positions of the diffraction lines of detected phases were marked: for the AB_2 phase by dots, for the ZrO_2 phase by the X figures. Broadening of the diffraction lines of the alloy after milling is extremely strong

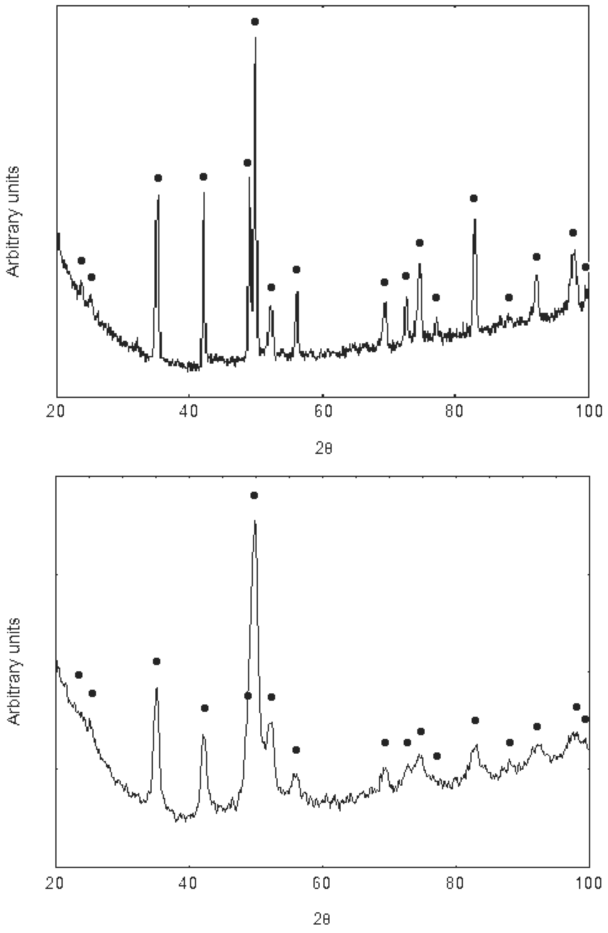

Fig. 2. X-ray diffraction patterns of SX 3 alloy: in basic state (higher) and after milling (lower). Positions of the diffraction lines of AB_5 phase were marked. Broadening of the diffraction lines after the milling process is increasing, but not as strong as in the SX 1 alloy

3. Discussion of results

The observation of diffraction patterns confirm that the crystal structure of the starting materials was in accordance with the assumptions. Both alloys had the composition of one-phase, despite of small amount of zirconium oxide, identified in the SX 1 sample. The diffraction patterns of the both alloys show strong differences between the diffraction line width of the alloy before and after milling. This indicates significant crystallite size reduction due to the milling process. Average diameters of the crystallites of the alloys, calculated from the diffraction line broadening, are: before the milling about 50 nm for the SX 1 sample, and about 100 nm for the SX 3 sample; after milling, respectively, about 4.5 nm and 20 nm.

The result for the SX 3 alloy after milling is obtained by the use of numerical separation of the overlapping profiles of its diffraction lines. From the comparison of those values, there can be observed that due to the milling process the average diameters of the alloys was extremely reduced, over ten-times for the SX 1 sample, and five-times for the SX 3 alloy.

Microanalysis shown that the starting material was monolithic and do not posses pores. It is characterized by high embrittlement. The evidence of this feature is the image of the surface of the crumbled materials (Fig. 3). Starting material is also characterized by significant non-homogeneity of the chemical composition (Tables 2 and 4). This feature significantly decreases as a result of high-energy milling (Tables 3 and 5).

Non-homogeneity can be additional reason of the diffraction line broadening. The examined areas, of the same crystal structure of the alloy, differ in chemical composition. Then those areas also differ slightly with the lattice parameters. Therefore, the position of diffraction line on the 2Θ scale is a function of the composition of an alloy. Because of that, the diffraction lines are broadening, due to the superposition of line, acquired from the examined areas with a different composition. It can be assumed that the average crystallite size of the starting material can be bigger then the value obtained from the Scherrer method. This assumption is not true for the material after milling because that material is found to be more homogenous.

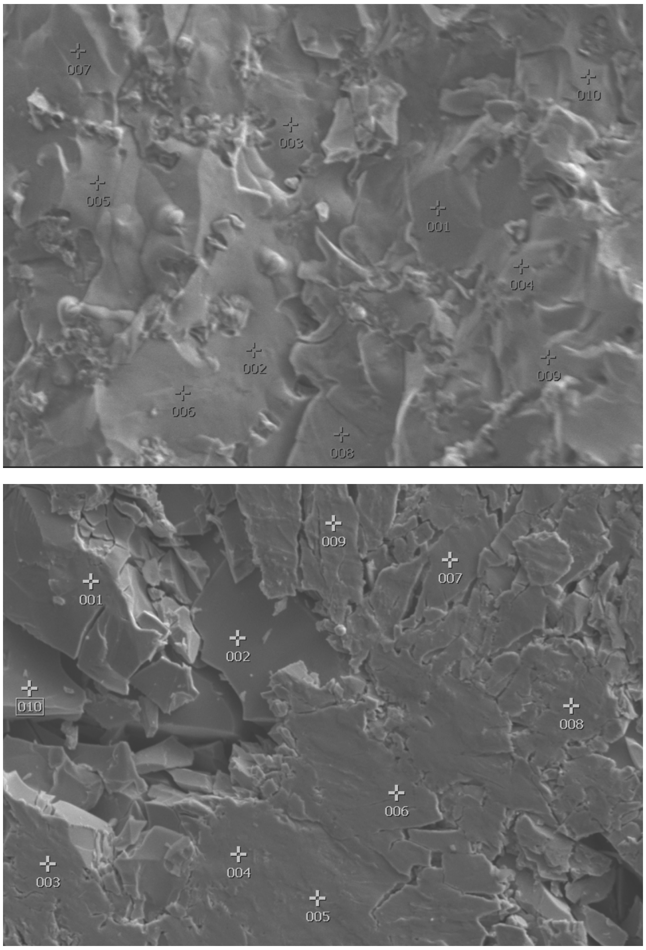

Fig. 3. Surface images of solid basic alloys: SX 1 (higher) and SX 3 (lower). Measurement points were marked. Secondary electron images, magnification 800 x

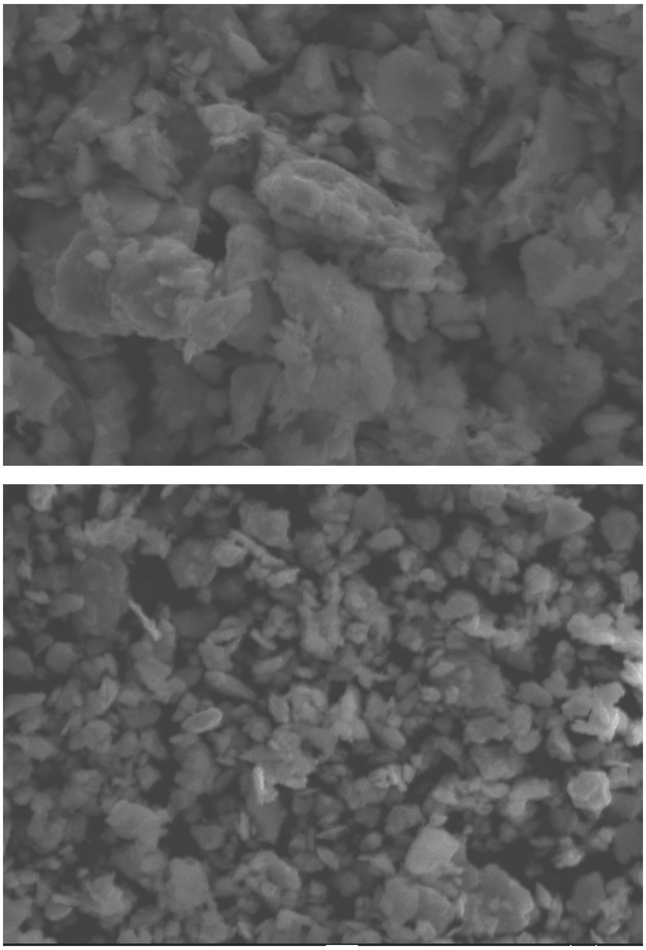

Fig. 4. Comparison of morphology of alloy powders particles: SX 1 (higher) and SX 3 (lower). Secondary electron images, magnification 5000 x

Average chemical composition of the alloys is defined by microanalysis. The analysis shows some differences between the measurements and theoretical assumptions. The SX 1 sample has reduced content of manganese, and the SX 3 reduced content of aluminum.

The morphology of obtained powders shows that the single grain is an agglomerate structure build from big amount of crystallites. These crystallites have average diameter of few μm for the SX 1 alloy, and of 1 μm for the SX 3. These assumptions are confirmed by the grain analysis presented in Table 6. The grain size, calculated by measurements of the surface (by the BET technique) and of the density, seems to be a true value for the size of particles of the powders. The measurement of grain size done by the laser diffraction on the other hand, gives the size value of the agglomerates.

After milling, the SX 3 alloy showed strong pyrophoric abilities, probably due to the large amount of misch metal in its composition. Several times the SX 3 alloy was self-igniting during the sample preparation. Because of that, the influence of the self-ignite on the sample composition was verified. It was observed, that during the self-ignite process, significant part of the alloy components was oxidizing. It was connected with full decompose of the intermetallic structure. The product acquired from this process is a mixture of oxides, mostly based on the structure of the CeO_2 and NiO, and nickel based solid solution.

Table 2.
Elementary composition of basic alloy SX 1 (mass %)

Element	**Ti**	**V**	**Cr**	**Mn**	**Ni**	**Zr**
Extent of contents	11.31-17.43	13.91-15.87	4,95-9.19	11.38-16.45	20.20-31.33	21.10-27.66
Average	**13.36**	**15.13**	**7.67**	**14.69**	**23.96**	**25.19**
Std. dev.	2.00	0.53	1.48	1.67	3.67	2.34

Table 3.
Elementary composition of alloy SX 1 after milling (mass %)

Element	**Ti**	**V**	**Cr**	**Mn**	**Ni**	**Zr**
Extent of contents	12.30-12.98	16.86-18.69	8.21-9.19	13.30-13.85	21.33-24.33	23.20-25.19
Average	**12.70**	**18.04**	**8.74**	**13.58**	**22.61**	**24.33**
Std. dev.	0.28	0.72	0.46	0.27	1.19	0.81

Table 4.
Elementary composition of basic alloy SX 3 (mass %)

Element	**Al**	**Mn**	**Co**	**Ni**	**La**	**Ce**
Extent of contents	0.61-1.17	3.38-15.95	11.90-14.76	36.92-48.52	10.10-15.13	19.82-20.89
Average	**0.86**	**7.65**	**13.68**	**45.41**	**11.98**	**20.42**
Std. dev.	0.22	4.01	0.73	3.62	1.28	0.33

Table 5.
Elementary composition of alloy SX 3 after milling (mass %)

Element	**Al**	**Mn**	**Co**	**Ni**	**La**	**Ce**
Extent of contents	0.42-1.34	5.13-7.07	13.49-14.24	45.96-47.55	11.45-12.46	19.68-21.00
Average	**0.94**	**6.12**	**13.97**	**46.71**	**11.98**	**20.30**
Std. dev.	0.38	0.72	0.26	0.60	0.42	0.57

Table 6.
Properties of investigated alloys

Alloy	SX 1, basic material, solid	SX 1, after milling, powder	SX 3, basic material, solid	SX 3, after milling, powder
Density, g/cm^3	6.817 ± 0.032	6.016 ± 0.006	7.985 ± 0.011	7.515 ± 0.007
BET surface area, m^2/g	about 0.03	8.742	about 0.04	2.695
Particle average diameter according to BET	-	0.10 μm	-	0.28 μm
Particle average diameter, median value	-	2.9 μm	-	1.6 μm
Particle average diameter, modal value	-	3.1 μm	-	1.9 μm
Fraction about diameter of particles < 0.3 μm	-	8.5 ± 0.5 mass %	-	19.0 ±1.0 mass %

Stronger agglomeration of the SX 1 alloy, despite the fact of the smaller crystallite size then the SX 3 sample, is probably an effect of the differences in the shape of the crystallites and its surface areas, between the alloys, and an effect of the differences in their clinging. The density drop of the both of powders, in compare to the solid material, is equal to 11.8% for the SX 1 alloy, and 5.9% for the SX 3. This density drop accurse because of the rise in amount of lattice defects, due to high-energy milling.

4. Conclusions

The presented data confirm obtaining the assumed objective, which was achieving hydrogen storage alloy of type AB_2 and AB_5 with an intended composition and structure, produced in a powder form, during a high-energy milling. Those materials, especially the pyrophoric SX 3 alloy, require though extreme caution during the milling, preparation and storage.

In both cases, the obtained materials were one-phase, chemically homogenous, nanocrystalline powders. Crystallite size for the SX 1 alloy was 4.5 nm. This value is several times smaller than the previously acquired value of few tens nm, with the same time of milling, but lower rpm rates [17]. Severe fragmentation of powder particles after milling was also observed. According to the results of the laser diffraction the alloys have average diameter of about 3 μm (SX 1 alloy) and below 2 μm (SX 3 alloy). Values calculated from the specific surface areas gave 0.10 μm and 0.28 μm, respectively.

The specific surface areas of the obtained powders were very high, especially the SX 1 alloy with the value of 8.74 m^2/g. The typical previously achieved specific surface areas were about 1.2 m^2/g or less [29,30], which also is a value few times smaller than the values presented in this paper. The application of the high milling energy, unreachable in earlier condition for ball milling, is leading to the improvement of the structure of obtained powders. The usable properties of the examined alloys are now a subject for studies, conducted by the authors.

Acknowledgements

This work was supported by the European Fund of Regional Development, the Project of No. POIG.01.01.02-00-015/09 “Advanced materials and technologies of their manufacturing”.

References

[1] G. Sandrock, K.J. Gross, G. Thomas, Effect of Ti-catalyst Content on the Reversible Hydrogen Storage Properties of the Sodum Alanates, Journal of Alloys and Compounds 339 (2002) 299-308.

[2] B. Friedrich, Large-Scale Production and Quality Assurance of Hydrogen Storage (Battery) Alloys, Journal of Materials Engineering and Performance 3 (1994) 37-46.

[3] E. David, An overview of advanced materials for hydrogen storage, Proceedings of the 13th International Scientific Conference “Achievements in Materials and Manufacturing Engineering” AMME'2005, Gliwice - Wisła, 2005, 95-98.

[4] D. Guixia, W. Borong, D. Jun, Z. Lei, Study on AB_5 Hydrogen Storage Alloy Used in Ni/MH Batteries for Electric Vehicles, Journal of Asian Electric Vehicles 3 (2005) 789-791.

[5] Y. Fukumoto, M. Miyamoto, M. Matsuoka, C. Iwakura, Effect of the stoichiometric ratio on electrochemical properties of hydrogen storage alloys for nickel-metal hydride batteries, Electrochimica Acta 40 (1995) 845-848.

[6] J.L. Lou, N. Cui, Effects of microencapsulation on the electrode behavior of Mg_2Ni-based hydrogen storage alloy in alkaline solution, Journal of Alloys and Compounds 264 (1998) 299-305.

[7] D.M. Kim, K.J. Jang, J.Y. Lee, A review on the development of AB_2-type Zr-based Laves phase hydrogen storage alloys for Ni-MH rechargeable batteries in the Korea Advanced Institute of Science and Technology, Journal of Alloys and Compounds 293-295 (1999) 583-592.

[8] R. Li, J.M. Wu, X.L. Wang, Effects of AB_5-type hydrogen storage alloy prepared by different techniques on the properties of MH/Ni batteries, Journal of Alloys and Compounds 311 (2000) 40-45.

[9] M. Kopczyk, A. Sierczyńska, E. Jankowska, W. Majchrzycki, Electrical characteristics of the prismatic high-power Ni/MH battery, Polish Journal of Chemical Technology 8/4 (2006) 67-69.

[10] C. Iwakura, T. Oura, H. Inoue, M. Matsuoka, Y. Yamamoto, Effect of alloy composition on hydrogen diffusion in the AB_5-type hydrogen storage alloys, Journal of Electroanalitical Chemistry 398 (1995) 37-41.

[11] C. Iwakura, T. Oura, H. Inoue, M. Matsuoka, Effects of substitution with foreign metals on the crystallographic, thermodynamic and electrochemical properties of AB_5-type hydrogen storage alloys, Electrochimica Acta 41 (1996) 117-121.

[12] L.Y. Zhang, Electrochemical characteristics of AB_5-type hydrogen storage alloys solidified at different cooling rates, Journal of Alloys and Compounds 293-295 (1999) 621-625.

[13] H. Pan, Y. Liu, M. Gao, Y. Zhu, Y. Lei, Q. Wang, An investigation on the structural and electrochemical properties of $La_{0.7}Mg_{0.3}(Ni_{0.85}Co_{0.15})_x$ (x=3.15-3.80) hydrogen storage electrode alloys, Journal of Alloys and Compounds 351 (2003) 228-234.

[14] H. Pan, Y. Liu, M. Gao, Y. Zhu, Y. Lei, The structural and electrochemical properties of $La_{0.7}Mg_{0.3}(Ni_{0.85}Co_{0.15})_x$ (x=3.0-5.0) hydrogen storage alloys, International Journal of Hydrogen Energy 28 (2003) 1219-1228.

[15] Z. Dong, Y. Wu, L. Ma, X. Shen, L. Wang, Electrochemical properties of $(La_{1-x}Ti_x)_{0.67}Mg_{0.33}Ni_{2.75}Co_{0.25}$ (x = 0-0.20 at.%) hydrogen storage alloys, Materials Research Bulletin 45 (2010) 256-261.

[16] www.fritsch.de/en/sample-preparation/products/milling/planetary-mills/.

[17] M. Jurczyk, Mechanical Alloying (Mechaniczna Synteza), Poznan University of Technology Press, Poznań, 2003 (in Polish).

[18] M. Staszewski, D. Kopyto, K. Becker, A. Wrona, J. Dworak, M. Kwarciński, The X-ray activated reduction of silver (I) solutions as a method for nanoparticles

manufacturing, Journal of Achievements in Materials and Manufacturing Engineering 28 (2008) 23-26.

[19] M. Czepelak, M. Staszewski, A. Wrona, M. Lis, M. Osadnik, Fabrication of nanostructured materials by high-pressure sintering, Archives of Materials Science and Engineering 30 (2008) 109-112.

[20] M. Makowiecka, E. Jankowska, I. Okońska, M. Jurczyk, Effect of Zr additions on the electrode characteristics of nanocrystaline TiNi-type hydrogen storage alloys, Journal of Alloys and Compounds 388 (2005) 303-307.

[21] A. Szajek, M. Makowiecka, E. Jankowska, M. Jurczyk, Electrochemical and electronic properties of nanocrystalline $TiNi_{1-x}M_x$ (M=Mg,Mn,Zr; x=0, 0.125, 0.250) ternary alloys, Journal of Alloys and Compounds 403 (2005) 323-328.

[22] E. Jankowska, M. Makowiecka, M. Jurczyk, Nickel-metal hydride battery using nanocrystalline TiFe-type hydrogen storage alloys, Journal of Alloys and Compounds 404-406 (2005) 691-693.

[23] E. David, Nanocrystalline magnesium and its properties of hydrogen sorption, Journal of Achievements in Materials and Manufacturing Engineering 20 (2007) 87-90.

[24] E. Jankowska, M. Makowiecka, M. Jurczyk, Electrochemical performance of sealed Ni-MH batteries using nanocrystalline TiNi-type hydride electrodes, Renewable Energy 33 (2008) 211-215.

[25] R. Mishima, H. Miyamura, T. Sakai, N. Kuriyama, H. Ishikawa, I. Uehara, Hydrogen storage alloys rapidly solidified by the melt-spinning method and their characteristics as metal hydride electrodes, Journal of Alloys and Compounds 192 (1993) 176-178.

[26] S. Ruggeri, L. Roué, J. Huot, R. Schulz, L. Aymard, J.M. Tarascon, Properties of mechanically alloyed Mg-Ni-Ti ternary hydrogen storage alloys for Ni-MH batteries, Journal of Power Sources 112 (2002) 547-556.

[27] S.F. Santos, A.L.M. Costa, J.F.R. de Castro, D.S. dos Santos, W.J. Botta, T.T. Ishikawa, Mechanical and Reactive Milling of a TiCrV BCC Solid Solution, Journal of Metastable and Nanocrystalline Materials 20-21 (2004) 291-296.

[28] Powder Diffraction File, JCPDS International Centre for Diffraction Data, Park Lane, USA, 2007.

[29] M. Ikoma, K. Komori, S. Kaida, Ch. Iwakura, Effect of alkali-treatment of hydrogen storage alloy on the degradation of Ni/MH batteries, Journal of Alloys and Compounds 284 (1999) 92-98.

[30] H.C. Lin, K.M. Lin, H.T. Chou, M.T. Eh, Effect of annealing and NaOH pretreatment on an $MnNi_{3.65}Al_{0.34}Mn_{0.27}Co_{0,74}$ hydrogen storage alloy, Journal of Alloys and Compounds 358 (2003) 281-287.